

Towards a High-Order Generalized Ghost Fluid Method.

Alexandre Noll Marques^a, Jean-Christophe Nave^b, Rodolfo Ruben Rosales^c

^a*Department of Aeronautics and Astronautics, Massachusetts Institute of Technology
Cambridge, MA 02139-4307*

^b*Department of Mathematics and Statistics, McGill University
Montreal, Quebec H3A 2K6, Canada*

^c*Department of Mathematics, Massachusetts Institute of Technology
Cambridge, MA 02139-4307*

Abstract

In this paper we present a method to treat interface jump conditions in Poisson problems that allows the use of standard “black box” solvers, without compromising accuracy. The basic idea of the new approach is similar to the Ghost Fluid Method (GFM). The GFM relies on corrections applied on nodes located across the interface for discretization stencils that straddle the interface. If the corrections are solution-independent, they can be moved to the right-hand-side (RHS) of the equations, producing a problem with the same linear system as if there were no jumps, only with a different RHS. With the “standard” approaches to computing the GFM correction terms, high accuracy is very hard (if not impossible) to achieve.

In this paper we generalize the GFM correction terms to a correction function, defined on a band around the interface. This function is then shown to be characterized as the solution to a PDE, with appropriate boundary conditions. This PDE can, in principle, be solved to any desired order of accuracy. As an example, we apply this new method to devise a 4th order accurate scheme for the Poisson equation with discontinuities in 2D. This scheme is based on the standard 9-point stencil discretization of the Poisson equation, a representation of the correction function in terms of bicubics, and a solution of the correction function PDE by a least squares minimization. Several applications of the method are presented to illustrate its robustness in dealing with a variety of interface geometries, its capability to capture sharp discontinuities, and its high convergence rate.

Keywords: Poisson equation, interface jump condition, Ghost Fluid method, Gradient augmented level set method, High accuracy, Hermite

cubic spline

PACS: 47.11-j, 47.11.Bc

2010 MSC: 76M20, 35N06

1. Introduction.

1.1. Motivation and background information.

In this paper we present a new and efficient method to solve the Poisson equation in the presence of discontinuities across an interface, with high order of accuracy. Solutions of the Poisson equation with discontinuities are of fundamental importance in the description of fluid flows separated by interfaces (*e.g.* the contact surfaces for immiscible multiphase fluids, or fluids separated by a membrane) and other multiphase diffusion phenomena. Over the last three decades, several methods have been developed to solve this problem numerically [1–14]. However, obtaining high order of accuracy still poses great challenges in terms of complexity and computational efficiency.

When the solution is known to be smooth, it is easy to obtain highly accurate finite-difference discretizations of the Poisson equation on a regular grid. Furthermore, these discretizations commonly yield symmetric and banded linear systems, which can be inverted quite efficiently [15]. On the other hand, when singularities occur (*e.g.* discontinuities) across internal interfaces, some of the regular discretization stencils will straddle the interface, which renders the whole procedure invalid.

Several strategies have been proposed to tackle this issue. Peskin [1] introduced the Immersed Boundary Method (IBM) [1, 10], in which the discontinuities are re-interpreted as additional (singular) source terms concentrated on the interface. These singular terms are then “regularized” and appropriately spread out over the regular grid — in a “thin” band enclosing the interface. This yields a first order scheme, and smeared discontinuities. In order to avoid this smearing of the interface information, LeVeque and Li [3] developed the Immersed Interface Method (IIM) [3, 4, 11, 13], which is a methodology to modify the discretization stencils, taking into consideration the discontinuities at their actual locations. The IIM guarantees second order accuracy and sharp discontinuities, but at the cost of added discretization complexity and loss of symmetry.

The new method advanced in this paper builds on the ideas introduced by the Ghost Fluid Method (GFM) [6–9, 12, 14]. The GFM is based on defining

both actual and “ghost” fluid variables at every node on a narrow band enclosing the interface. The ghost variables work as extensions of the actual variables across the interface — the solution on each side of the interface is assumed to have a smooth extension into the other side. This allows the use of a standard discretizations everywhere in the domain. In most GFM versions, the ghost values are written as the actual values, plus corrections that are independent of the underlying solution to the Poisson problem. Hence, the corrections can be pre-computed, and moved into the source term for the equation. In this fashion the GFM yields the same linear system as the one produced by the problem without an interface, except for changes in the right-hand-side (sources) only, which can then be inverted just as efficiently.

The key difficulty in the GFM is the calculation of the correction terms, since the overall accuracy of the scheme depends heavily on the quality of the assigned ghost values. In Refs. [6–9, 12] the authors develop first order accurate approaches to deal with discontinuities. In the present work, so as to obtain high order accuracy, we first generalize the GFM correction term (at each ghost point) concept to that of a correction function defined on a narrow band enclosing the interface. This correction function is then shown to be characterized as the solution to a PDE, with appropriate boundary conditions on the interface — see § 4. Thus, at least in principle, one can calculate the correction function to any order of accuracy, by designing algorithms to solve the PDE that defines it. In this paper we present an example of a 4th order accurate scheme (to solve the Poisson equation, with discontinuities across interfaces, in 2D) developed using this general framework. Two key points (see §5) in the scheme development are

1. The PDE problem defining the correction function is solved using a least squares minimization approach. This provides a flexible approach that allows the development of a robust scheme that can deal with the geometrical complications of the placement of the regular grid stencils relative to the interface. Furthermore, this approach is easy to generalize to 3D, or to even higher orders of accuracy.
2. To achieve 4th order accuracy, the interface must be represented with corresponding accuracy. To this end, we use a Gradient-Augmented Level-Set approach [16] — see § 1.3 below.

1.2. Other related work.

It is relevant to note other developments to solve the Poisson equation under similar circumstances — multiple phases separated by interfaces —

but with different interface conditions. The Poisson problem with Dirichlet boundary conditions, on an irregular boundary embedded in a regular grid, has been solved to second order of accuracy using fast Poisson solvers [17], finite volume [5], and finite differences [18–21] approaches. In particular, Gibou *et al.* [19] and Jomaa and Macaskill [20] have shown that it is possible to obtain symmetric discretizations of the embedded Dirichlet problem, up to second order of accuracy. Gibou and Fedkiw [21] have developed a fourth order accurate discretization of the problem, at the cost of giving up symmetry. More recently, the same problem has also been solved, to second order of accuracy, in non-graded adaptive Cartesian grids by Chen *et al.* [22]. Furthermore, the embedded Dirichlet problem has been shown to be closely related to the Stefan problem modeling dendritic growth, as described in Refs. [23, 24].

1.3. Interface representation.

Another issue of primary importance to multiphase problems is the representation of the interface (and its tracking in unsteady cases). Some authors (see Refs. [1, 17, 18]) choose to represent the interface explicitly, by tracking interface particles. The location of the neighboring particles is then used to produce local interpolations (*e.g.* splines), which are then applied to compute geometric information — such as curvature and normal directions. Although this approach can be quite accurate, it requires special treatment when the interface undergoes either large deformations or topological changes — such as merger or split. Even though we are not concerned with these issues in this paper, we elected to adopt an implicit representation, to avoid complications in future applications. In an implicit representation, the interface is given as the zero level of a function that is defined everywhere in the regular grid — the level set function. To be more precise, we adopted the Gradient-Augmented Level-Set (GA-LS) method [16]. With this extension of the level-set method, we can obtain highly accurate representations of the interface, and other geometric information, using local grid information only.

1.4. Organization of the paper.

The remainder of the paper is organized as follows. In § 2 we introduce the Poisson problem that we seek to solve. In § 3 the basic idea behind the solution method, and its relationship to the GFM, are explored. The generalization of the GFM approach to the use of a correction function defined by a PDE problem is done next, in § 4. In § 5 we apply this new framework to

build a 4th order accurate scheme in 2D, which is described in detail there. Next, in § 6 we demonstrate the robustness and accuracy of the 2D scheme by applying it to several example problems. Finally, § 7 has the conclusions.

2. Definition of the problem.

Our objective is to solve Poisson’s equation in a domain Ω in which the solution is discontinuous across a co-dimension 1 interface Γ , which divides the domain into the subdomains Ω^+ and Ω^- , as in Fig. 1. We use the notation u^+ and u^- to denote the solution in each of the subdomains. Let the discontinuities across Γ be given in terms of two functions defined on the interface: $a = a(\vec{x})$ for the jump in the function values, and $b = b(\vec{x})$ for the jump in the normal derivatives. Furthermore, assume Dirichlet boundary conditions on the “outer” boundary $\partial\Omega$ (see Fig. 1). Thus the problem to be solved is

$$\nabla^2 u(\vec{x}) = f(\vec{x}) \quad \text{for } \vec{x} \in \Omega, \quad (1a)$$

$$[u]_\Gamma = a(\vec{x}) \quad \text{for } \vec{x} \in \Gamma, \quad (1b)$$

$$[u_n]_\Gamma = b(\vec{x}) \quad \text{for } \vec{x} \in \Gamma, \quad (1c)$$

$$u(\vec{x}) = g(\vec{x}) \quad \text{for } \vec{x} \in \partial\Omega, \quad (1d)$$

where

$$[u]_\Gamma = u^+(\vec{x}) - u^-(\vec{x}) \quad \text{for } \vec{x} \in \Gamma, \quad (2a)$$

$$[u_n]_\Gamma = u_n^+(\vec{x}) - u_n^-(\vec{x}) \quad \text{for } \vec{x} \in \Gamma. \quad (2b)$$

Throughout this paper, $\vec{x} = (x_1, x_2, \dots) \in \mathbb{R}^\nu$ is the spatial vector (where $\nu = 2$, or $\nu = 3$), and ∇^2 is the Laplacian operator defined by

$$\nabla^2 = \sum_{i=1}^{\nu} \frac{\partial^2}{\partial x_i^2}. \quad (3)$$

Furthermore,

$$u_n = \hat{n} \cdot \vec{\nabla} u = \hat{n} \cdot (u_{x_1}, u_{x_2}, \dots) \quad (4)$$

denotes the derivative of u in the direction of \hat{n} , the unit vector normal to the interface Γ pointing towards Ω^+ (see Fig. 1).

It is important to note that our method focuses on the discretization of the problem in the vicinity of the interface only. Thus, the method is compatible with any set of boundary conditions on $\partial\Omega$, not just Dirichlet.

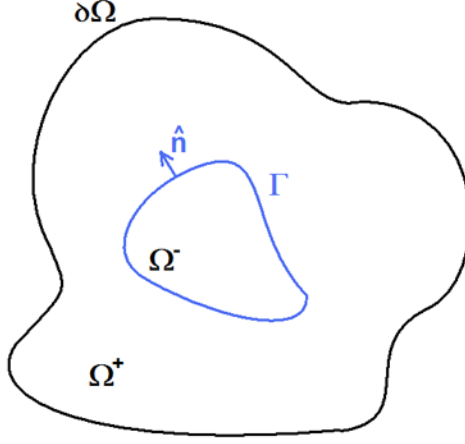


Figure 1: Example of a domain Ω , with an interface Γ .

3. Solution method – the basic idea.

To achieve the goal of efficient high order discretizations of Poisson equation in the presence of discontinuities, we build on the idea of the Ghost Fluid Method (GFM). In essence, we use a standard discretization of the Laplace operator (on a domain without an interface Γ) and modify the right-hand-side (RHS) to incorporate the jump conditions across Γ . Thus, the resulting linear system can be inverted as efficiently as in the case of a solution without discontinuities.

Let us first illustrate the key concept in the GFM with a simple example, involving a regular grid and the standard second order discretization of the 1D analog of the problem we are interested in. Thus, consider the problem of discretizing the equation $u_{xx} = f(x)$ in some interval $\Omega = \{x : x_L < x < x_R\}$, where u is discontinuous across some point x_Γ — hence Ω^+ (respectively Ω^-) is the domain $x_L < x < x_\Gamma$ (respectively $x_\Gamma < x < x_R$). Then, see Fig. 2, when trying to approximate u_{xx} at a grid point x_i such that $x_i < x_\Gamma < x_{i+1}$, we would like to write

$$u_{xx_i}^+ \approx \frac{u_{i-1}^+ - 2u_i^+ + u_{i+1}^+}{h^2}, \quad (5)$$

where $h = x_{j+1} - x_j$ is the grid spacing. However, we do not have information

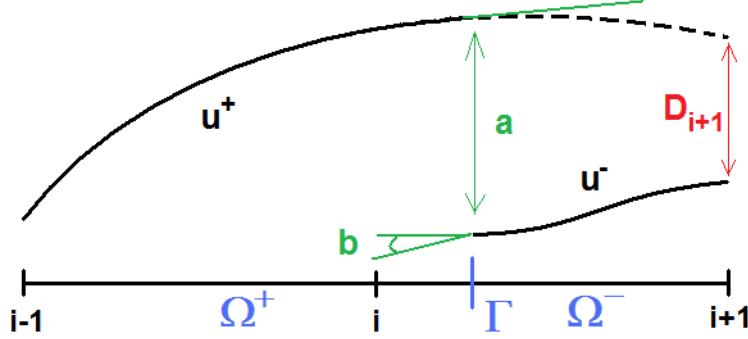


Figure 2: Example in 1D of a solution with a jump discontinuity.

on u_{i+1}^+ , but rather on u_{i+1}^- . Thus, the idea is to estimate a correction for u_{i+1}^- , to recover u_{i+1}^+ , such that Eq. (5) can be applied:

$$u_{xx_i}^+ \approx \frac{u_{i-1}^+ - 2u_i^+ + \overbrace{(u_{i+1}^- + D_{i+1})}^{u_{i+1}^+}}{h^2}, \quad (6)$$

where $D_{i+1} = u_{i+1}^+ - u_{i+1}^-$ is the correction term. Now we note that, if D_{i+1} can be written as a correction that is independent on the solution u , then it can be moved to the RHS of the equation, and absorbed into f . That is

$$\frac{u_{i-1}^+ - 2u_i^+ + u_{i+1}^-}{h^2} = f_i - \frac{D_{i+1}}{h^2}. \quad (7)$$

This allows the solution of the problem with prescribed discontinuities using the same discretization as the one employed to solve the simpler problem without an interface — which leads to a great efficiency gain.

Remark 1. The error in estimating D is crucial in determining the accuracy of the final discretization. Liu, Fedkiw, and Kang [9] introduced a dimension-by-dimension linear extrapolation of the interface jump conditions, to get a first order approximation for D . Our new method is based on generalizing the idea of a correction term to that of a *correction function*, for which we can write an equation. One can then obtain high accuracy representations for D by solving this equation, without the complications into which dimension-by-dimension (with Taylor expansions) approaches run into. ♣

Remark 2. An additional advantage of the correction function approach is that D can be calculated at any point near the interface Γ . Hence it can be used with any finite differences discretization of the Poisson equation, without regard to the particulars of its stencil (as would be the case with any approach based on Taylor expansions). ♣

4. The correction function and the equation defining it.

As mentioned earlier, the aim here is to generalize the correction term concept to that of a *correction function*, and then to find an equation (a PDE, with appropriate boundary conditions) that uniquely characterizes the *correction function*. Then, at least in principle, one can design algorithms to solve the PDE in order to obtain solutions to the *correction function* of any desired order of accuracy.

Let us begin by considering a small region Ω_Γ enclosing the interface Γ , defined as the set of all the points within some distance \mathcal{R} of Γ , where \mathcal{R} is of the order of the grid size h . As we will see below, we would like to have \mathcal{R} as small as possible. On the other hand, Ω_Γ has to include all the points where the GFM requires corrections to be computed, which means¹ that \mathcal{R} cannot be smaller than $\sqrt{2}h$. In addition, algorithmic considerations (to be seen later) force \mathcal{R} to be slightly larger than this last value.

Next, we assume we that can extrapolate both u^+ and u^- , so that they are valid everywhere within Ω_Γ , in such a way that they satisfy the Poisson equations

$$\nabla^2 u^+(\vec{x}) = f^+(\vec{x}) \quad \text{for } \vec{x} \in \Omega_\Gamma, \quad (8a)$$

$$\nabla^2 u^-(\vec{x}) = f^-(\vec{x}) \quad \text{for } \vec{x} \in \Omega_\Gamma, \quad (8b)$$

where f^+ and f^- are smooth enough (see remark 3 below) extensions of the source term f to Ω_Γ . In particular, notice that the introduction of f^+ and f^- allows for the possibility of the source term changing (*i.e.* a discontinuous source term) across Γ . The *correction function* is then defined by $D(\vec{x}) = u^+(\vec{x}) - u^-(\vec{x})$.

Taking the difference between the equations in (8), and using the jump

¹For the particular discretization of the Laplace operator that we use in this paper.

conditions (1b-1c), yields

$$\nabla^2 D(\vec{x}) = f^+(\vec{x}) - f^-(\vec{x}) = f_D(\vec{x}) \quad \text{for } \vec{x} \in \Omega_\Gamma, \quad (9a)$$

$$D(\vec{x}) = a(\vec{x}) \quad \text{for } \vec{x} \in \Gamma, \quad (9b)$$

$$D_n(\vec{x}) = b(\vec{x}) \quad \text{for } \vec{x} \in \Gamma. \quad (9c)$$

This achieves the aim of having the *correction function* defined by a set of equations, with some provisos — see remark 4 below. Note that:

1. If $f^+(\vec{x}) = f^-(\vec{x})$, for $\vec{x} \in \Omega_\Gamma$, then $f_D(\vec{x}) = 0$, for $\vec{x} \in \Omega_\Gamma$.
2. Equation (9c) imposes the true jump condition in the normal direction, whereas some versions of the GFM rely on a dimension-by-dimension approximation of this condition (see Ref. [9]).

Remark 3. The smoothness requirement on f^+ and f^- is tied up to how accurate an approximation to the correction term D is needed. For example, if a 4th order algorithm is used to find D , this will (generally) necessitate D to be at least C^4 for the errors to actually be 4th order. Hence, in this case, $f_D = f^+ - f^-$ must be C^2 . ♣

Remark 4. Equation (9) is an elliptic Cauchy problem for D in Ω_Γ . In general, such problems are ill-posed. However, we are seeking for solutions within the context of a numerical approximation where

- (a) There is a frequency cut-off in both the data $a = a(\vec{x})$ and $b = b(\vec{x})$, and the description of the curve Γ .
- (b) We are interested in the solution only a small distance away from the interface Γ , where this distance vanishes simultaneously with the inverse of the cut-off frequency in point (a).

What (a) and (b) mean is that the arbitrarily large growth rate for arbitrarily small perturbations, which is responsible for the ill-posedness of the Cauchy problem in Eq. (9), does not occur within the special context where we need to solve the problem. This large growth rate does not occur because, for the solutions of the Poisson equation, the growth rate for a perturbation of wave number $0 < k < \infty$ along some straight line, is given by $e^{2\pi kd}$ — where d is the distance from the line. However, by construction, in the case of interest to us kd is bounded. ♣

Remark 5. Let us be more precise, and define a number characterizing how well posed the discretized version of Eq. (9) is, by

$$\alpha = \text{largest growth rate possible,}$$

where growth is defined relative to the size of a perturbation to the solution on the interface. This number is determined by \mathcal{R} (the “radius” of Ω_Γ) as the following calculation shows: First of all, there is no loss of generality in assuming that the interface is flat, provided that the numerical grid is fine enough to resolve Γ . In this case, let us introduce an orthogonal coordinate system \vec{y} on Γ , and let d be the signed distance to Γ (say, $d > 0$ in Ω^-). Expanding the perturbations in Fourier modes along the interface, the typical mode has the form

$$\varphi_{\vec{k}} = e^{2\pi i \vec{k} \cdot \vec{y} \pm 2\pi k d},$$

where \vec{k} is the Fourier wave vector, and $k = |\vec{k}|$. The shortest wave-length that can be represented on a grid with mesh size $0 < h \ll 1$ corresponds to $k = k_{\max} = 1/(2h)$. Hence, we obtain the estimate

$$\alpha \approx e^{\pi \mathcal{R}_c / h}$$

for the maximum growth rate. ♣

Remark 6. Clearly, α is intimately related to the condition number for the discretized problem — see § 5. In fact, at leading order, the two numbers should be (roughly) proportional to each other — with a proportionality constant that depends on the details of the discretization. For the discretization used in this paper (described further below), $\sqrt{2}h \leq \mathcal{R} \leq 2\sqrt{2}h$, which leads to the rough estimate $85 < \alpha < 7,200$. On the other hand, the observed condition numbers vary between 5,000 and 10,000. Hence, the actual condition numbers are only slightly higher than α for the ranges of grid sizes h that we used (we did not explore the asymptotic limit $h \rightarrow 0$). ♣

Remark 7. Eq. (9) depends on the known inputs for the problem only. Namely: f^+ , f^- , a , and b . Consequently D does not depend on the solution u . Hence, after solving for D , we can use a discretization for u that does not involve the interface: Whenever u is discontinuous, we evaluate D where the correction is needed, and transfer these values to the RHS. ♣

Remark 8. When developing an algorithm for a linear Cauchy problem, such as the one in Eq. (9), the two key requirements are consistency and stability. In particular, when the solution depends on the “initial conditions” globally, stability (typically) imposes stringent constraints on the “time” step for any local (explicit) scheme. This would seem to suggest that, in order to solve Eq. (9), a “global” (involving the whole domain Ω_Γ) method will be needed. This, however, is not true: because we need to solve Eq. (9) for one “time” step only — *i.e.* within an $\mathcal{O}(h)$ distance from Γ , stability is not relevant. Hence, consistency is enough, and a fully local scheme is possible. In the algorithm described in § 5 we found that, for (local) quadrangular patches, the Cauchy problem leads to a well behaved algorithm when the length of the interface contained in each patch is of the same order as the diagonal length of the patch. This result is in line with the calculation in remark 5: we want to keep the “wavelength” (along Γ) of the perturbations introduced by the discretization as long as possible. In particular, this should then minimize the condition number for the local problems — see remark 6. ♣

5. A 4th Order Accurate Scheme in 2D.

5.1. Overview.

In this section we use the general ideas presented earlier, to develop a specific example of a 4th order accurate scheme in 2D. Before proceeding with an in-depth description of the scheme, we highlight a few key points:

- (a) We discretize Poisson’s equation using a compact 9-point stencil. Compactness is important since it is directly related to the size of ℓ_c , which has a direct impact on the problem’s conditioning — see remarks 4 – 6.
- (b) We approximate D using bicubic interpolations (bicubics), each valid in a small neighborhood $\Omega_\Gamma^{i,j}$ of the interface. This guarantees local 4th order accuracy with only 12 interpolation parameters — see [16]. Each $\Omega_\Gamma^{i,j}$ corresponds to a point in the grid at which the standard discretization of Poisson’s equation involves a stencil that straddles the interface Γ .
- (c) The domains $\Omega_\Gamma^{i,j}$ are rectangular regions, each enclosing a portion of Γ , and all the nodes where D is needed to complete the discretization of the Poisson equation at the (i, j) -th stencil. Each is a sub-domain of Ω_Γ .
- (d) Starting from (b) and (c), we design a local solver that provides an approximation to D inside each domain $\Omega_\Gamma^{i,j}$.

- (e) The interface Γ is represented using the Gradient-Augmented Level-Set approach — see [16]. This guarantees a local 4th order representation of the interface, as required to keep the overall accuracy of the scheme.
- (f) In each $\Omega_{\Gamma}^{i,j}$, we solve the PDE in (9) in a least square sense. Namely: First we define an appropriate positive quadratic integral quantity J_P for which the solution is a minimum (actually, zero). Next we substitute the bicubic approximation for the solution into J_P , and discretize the integrals using Gaussian quadrature. Finally, we find the bicubic parameters by minimizing the discretized J_P .

Remark 9. Solving the PDE in a least square sense is crucial, since an algorithm is needed that can deal with the myriad ways in which the interface Γ can be placed relative to the fixed rectangular grid used to discretize Poisson’s equation. This approach provides a scheme that: (i) Is robust with respect to the details of the interface geometry. (ii) Has a formulation that is (essentially) dimension independent — no fundamental changes from 2D to 3D. (iii) Has a clear theoretical underpinning that allows extensions to higher orders, or to other discretizations of the Poisson equation. ♣

5.2. Standard Stencil.

We use the standard 4th order accurate 9-point discretization of Poisson’s equation:²

$$L^5 u_{i,j} + \frac{1}{12} (h_x^2 + h_y^2) \hat{\partial}_{xxyy} u_{i,j} = f_{i,j} + \frac{1}{12} (h_x^2 (f_{xx})_{i,j} + h_y^2 (f_{yy})_{i,j}), \quad (10)$$

where L^5 is the second order 5-point discretization of the Laplace operator:

$$L^5 u_{i,j} = \frac{u_{i+1,j} - 2u_{i,j} + u_{i-1,j}}{h_y^2} + \frac{u_{i,j+1} - 2u_{i,j} + u_{i,j-1}}{h_x^2}, \quad (11)$$

and

$$\hat{\partial}_{xxyy} u_{i,j} = \frac{1}{(h_x h_y)^2} \left[(u_{i+1,j+1} + u_{i+1,j-1} + u_{i-1,j+1} + u_{i-1,j-1}) - 2(u_{i+1,j} + u_{i-1,j} + u_{i,j+1} + u_{i,j-1}) + 4u_{i,j} \right]. \quad (12)$$

²Notice that here we allow for the possibility of different grid spacings in each direction.

The terms $(f_{xx})_{i,j}$ and $(f_{yy})_{i,j}$ may be given analytically (if known), or computed using second order accurate centered differences.

In the absence of discontinuities, Eq. (10) provides a compact 4th order accurate representation of Poisson's equation. In the vicinity of the discontinuities at the interface Γ , we define an appropriate domain $\Omega_{\Gamma}^{i,j}$, and compute the correction terms necessary to Eq. (10) — as described in detail next.

To understand how the correction terms affect the discretization, let us consider the situation depicted in Fig. 3. In this case, the node (i, j) lies in Ω^+ while the nodes $(i+1, j)$, $(i+1, j+1)$, and $(i, j+1)$ are in Ω^- . Hence, to be able to use Eq. (10), we need to compute $D_{i+1,j}$, $D_{i+1,j+1}$, and $D_{i,j+1}$.

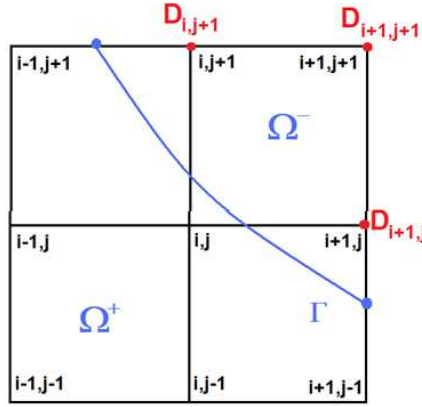


Figure 3: The 9-point compact stencil next to the interface Γ .

After having solved for D where necessary (see § 5.3 and § 5.4), we modify Eq. (10) and write

$$L^5 u_{i,j} + \frac{1}{12} (h_x^2 + h_y^2) \hat{\partial}_{xxyy} u_{i,j} = f_{i,j} + \frac{1}{12} (h_x^2 (f_{xx})_{i,j} + h_y^2 (f_{yy})_{i,j}) + C_{i,j}, \quad (13)$$

which differs from Eq. (10) by the terms $C_{i,j}$ on the RHS only. Here the $C_{i,j}$ are the GFM correction terms needed to complete the stencil across the

discontinuity at Γ . In the particular case illustrated by Fig. 3, we have

$$C_{i,j} = \left[\frac{1}{6} \frac{(h_x^2 + h_y^2)}{(h_x h_y)^2} - \frac{1}{h_y^2} \right] D_{i+1,j} + \left[\frac{1}{6} \frac{(h_x^2 + h_y^2)}{(h_x h_y)^2} - \frac{1}{h_x^2} \right] D_{i,j+1} - \frac{1}{12} \frac{(h_x^2 + h_y^2)}{(h_x h_y)^2} D_{i+1,j+1}. \quad (14)$$

Similar formulas apply for the other possible arrangements of the Poisson's equation stencil relative to the interface Γ .

5.3. Definition of $\Omega_\Gamma^{i,j}$.

As follows from the arguments in § 4, there is some arbitrariness on how to define $\Omega_\Gamma^{i,j}$. The requirements are

- (i) $\Omega_\Gamma^{i,j}$ should be a rectangle with its sides parallel to the grid lines.
- (ii) $\Omega_\Gamma^{i,j}$ should be small, since the problem's condition number increases exponentially with the distance from Γ — see remarks 5 and 6.
- (iii) $\Omega_\Gamma^{i,j}$ should contain all the nodes where D is needed. For the example in Fig. 3, we need to know $D_{i+1,j+1}$, $D_{i+1,j}$, and $D_{i,j+1}$. Hence, in this case, $\Omega_\Gamma^{i,j}$ should include the nodes $(i+1, j+1)$, $(i+1, j)$, and $(i, j+1)$.
- (iv) $\Omega_\Gamma^{i,j}$ should contain a segment of Γ , with a length that is as large as possible — *i.e.* comparable to the length of the diagonal of $\Omega_\Gamma^{i,j}$. This follows from the calculation in remark 5, which indicates that the wavelength of the perturbations (along Γ) introduced by the discretization should be as long as possible. This should then minimize the condition number for the local problem — see remark 6.

The requirement in (i) is for algorithmic convenience only, and does not arise from any particular argument in § 4. Thus, in principle, this convenience could be traded for some improvement in the other items — hence in the condition numbers for the local problems. However, for simplicity, in this paper we enforce (i): As explained earlier (see remark 9), we solve Eq. (9) in a least squares sense. Hence integrations over $\Omega_\Gamma^{i,j}$ are required. It is thus useful to keep $\Omega_\Gamma^{i,j}$ as simple as possible.

With the points above in mind, we define $\Omega_\Gamma^{i,j}$ as the smallest rectangle that satisfies conditions (i), (iii) and (iv) — thus condition (ii) follows automatically. Hence $\Omega_\Gamma^{i,j}$ is defined by the following three easy steps:

1. Find the coordinates $(x_{\min_\Gamma}, x_{\max_\Gamma})$ and $(y_{\min_\Gamma}, y_{\max_\Gamma})$ of the smallest rectangle satisfying condition (i), which completely encloses the section of the interface Γ contained by the region covered by the 9-point stencil.
2. Find the coordinates (x_{\min_D}, x_{\max_D}) and (y_{\min_D}, y_{\max_D}) of the smallest rectangle satisfying condition (i), which completely encloses all the nodes at which D needs to be known.
3. Then $\Omega_\Gamma^{i,j}$ is the smallest rectangle that encloses the two previous rectangles. Its edges are given by

$$x_{\min} = \min(x_{\min_\Gamma}, x_{\min_D}), \quad (15a)$$

$$x_{\max} = \max(x_{\max_\Gamma}, x_{\max_D}), \quad (15b)$$

$$y_{\min} = \min(y_{\min_\Gamma}, y_{\min_D}), \quad (15c)$$

$$y_{\max} = \max(y_{\max_\Gamma}, y_{\max_D}). \quad (15d)$$

Figure 4 shows an example of $\Omega_\Gamma^{i,j}$ defined using these specifications.

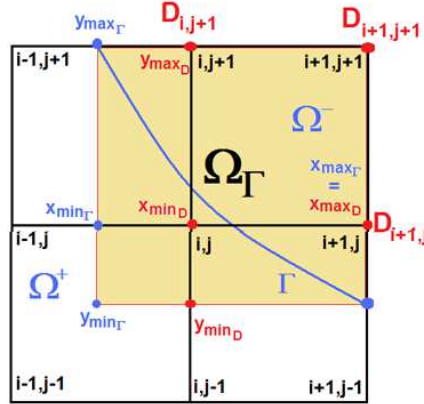


Figure 4: The set $\Omega_\Gamma^{i,j}$ for the situation in Fig. 3.

Remark 10. Notice that for each node next to the interface we construct a domain $\Omega_\Gamma^{i,j}$. When doing so, we allow the domains to overlap. For example, the domain $\Omega_\Gamma^{i,j}$ shown in Fig. 4 is used to determine $C_{i,j}$. It should be clear that $\Omega_\Gamma^{i-1,j+1}$ (used to determine $C_{i-1,j+1}$), and $\Omega_\Gamma^{i+1,j-1}$ (used to determine $C_{i+1,j-1}$), each will overlap with $\Omega_\Gamma^{i,j}$.

The consequence of these overlaps is that different computed values for D at the same node can (in fact, will) happen — depending on which domain is used to solve the local Cauchy problem. However, because we solve for D — within each $\Omega_{\Gamma}^{i,j}$ — to 4th order accuracy, any differences that arise from this multiple definition of D lie within the order of accuracy of the scheme. Since it is convenient to keep the computations local, the values of D resulting from the domain $\Omega_{\Gamma}^{i,j}$, are used to evaluate the correction term $C_{i,j}$. ♣

5.4. Solution of the Local Cauchy Problem.

Since we use a 4th order accurate discretization of the Poisson problem, we need to find D with 4th order errors (or better) to keep the overall accuracy of the scheme — see §5.7. Hence we approximate D using cubic Hermite splines (bicubic interpolants in 2D), which guarantees 4th order accuracy — see [16]. Note also that, even though the example scheme developed here is for 2D, this representation can be easily extended to any number of dimensions.

Given a choice of basis functions,³ we solve the local Cauchy problem defined in Eq. (9) in a least squares sense, using a minimization procedure. Since we do not have boundary conditions, but interface conditions, we must resort to a minimization functional that is different from the standard one associated with the Poisson equation. Thus we impose the Cauchy interface conditions by using a penalization method. The functional to be minimized is then

$$\begin{aligned} J_P = & (\ell_c^{i,j})^3 \int_{\Omega_{\Gamma}^{i,j}} [\nabla^2 D(\vec{x}) - f_D(\vec{x})]^2 dV \\ & + c_P \int_{\Gamma \cap \Omega_{\Gamma}^{i,j}} [D(\vec{x}) - a(\vec{x})]^2 dS \\ & + c_P (\ell_c^{i,j})^2 \int_{\Gamma \cap \Omega_{\Gamma}^{i,j}} [D_n(\vec{x}) - b(\vec{x})]^2 dS, \end{aligned} \quad (16)$$

where $c_P > 0$ is the penalization coefficient used to enforce the interface conditions, and $\ell_c^{i,j} > 0$ is a characteristic length associated with $\Omega_{\Gamma}^{i,j}$ — we used the shortest side length. Clearly J_P is a quadratic functional whose minimum (zero) occurs at the solution to Eq. (9).

³The basis functions that we use for the bicubic interpolation can be found in § Appendix A.

In order to compute D in the domain $\Omega_{\Gamma}^{i,j}$, its bicubic representation is substituted into the formula above for J_P , with the integrals approximated by Gaussian quadratures — in this paper we used six quadrature points for the 1D line integrals, and 36 points for the 2D area integrals. The resulting discrete problem is then minimized. Because the bicubic representation for D involves 12 basis polynomials, the minimization problem produces a 12×12 (self-adjoint) linear system.

Remark 11. We explored the option of enforcing the interface conditions using Lagrange multipliers. While this second approach yields good results, our experience shows that the penalization method is better. ♣

Remark 12. The scaling using $\ell_c^{i,j}$ in Eq. (16) is so that all the three terms in the definition of J_p behave in the same fashion as the size of $\Omega_{\Gamma}^{i,j}$ changes with (i, j) , or when the computational grid is refined.⁴ This follows because we expect that

$$\begin{aligned}\nabla^2 D - f &= \mathcal{O}(\ell_c^2), \\ D - a &= \mathcal{O}(\ell_c^4), \\ D_n - b &= \mathcal{O}(\ell_c^3).\end{aligned}$$

Hence each of the three terms in Eq. (16) should be $\mathcal{O}(\ell_c^9)$. ♣

Remark 13. Once all the terms in Eq. (16) are guaranteed to scale the same way with the size of $\Omega_{\Gamma}^{i,j}$, the penalization coefficient c_P should be selected so that the three terms have (roughly) the same size for the numerical solution (they will, of course, not vanish). In principle, c_P could be determined from knowledge of the fourth order derivatives of the solution, which control the error in the numerical solution. This approach does not appear to be practical. A simpler method is based on the observation that c_P should not depend on the grid size (at least to leading order, and we do not need better than this). Hence it can be determined empirically from a low resolution calculation. In the examples in this paper we found that $c_P \approx 50$ produced good results. ♣

⁴The scaling also follows from dimensional consistency.

Remark 14. A more general version of J_P in Eq. (16) would involve different penalization coefficients for the two line integrals, as well as the possibility of these coefficients having a dependence on the position along Γ of $\Omega_\Gamma^{i,j}$. These modifications could be useful in cases where the solution to the Poisson problem has large variations — *e.g.* a very irregular interface Γ , or a complicated forcing f . ♣

5.5. Computational Cost.

We can now infer something about the cost of the present scheme. To start with, let us denote the number of nodes in the x and y directions by

$$N_x = \frac{1}{h_x} + 1, \quad N_y = \frac{1}{h_y} + 1, \quad (17)$$

assuming a 1 by 1 computational square. Hence, the total number of degrees of freedom is $M = N_x N_y$. Furthermore, the number of nodes adjacent to the interface is $\mathcal{O}(M^{1/2})$, since the interface is a 1D entity.

The discretization of Poisson’s equation results in a $M \times M$ linear system. Furthermore, the present method produces changes only on the RHS of the equations. Thus, the basic cost of inverting the system is unchanged from that of inverting the system resulting from a problem without an interface Γ . Namely: it varies from $\mathcal{O}(M)$ to $\mathcal{O}(M^2)$, depending on the solution method.

Let us now consider the computational cost added by the modifications to the RHS. As presented above, for each node adjacent to the interface, we must construct $\Omega_\Gamma^{i,j}$, compute the integrals that define the local 12×12 linear system, and invert it. The cost associated with these tasks is constant: it does not vary from node to node, and it does not change with the size of the mesh. Consequently the resulting additional cost is a constant times the number of nodes adjacent to the interface. Hence it scales as $M^{1/2}$. Because of the (relatively large) coefficient of proportionality, for small M this additional cost can be comparable to the cost of inverting the Poisson problem. Obviously, this extra cost becomes less significant as M increases.

5.6. Interface Representation.

The framework needed to solve the local Cauchy problems has been (almost) entirely described above. There is just one more issue that deserves some attention: the correct representation of the interface. In the present work, we do not assume that we know the interface exactly, since this is what one can expect in general.

To guarantee the accuracy of the solution for D , the interface conditions must be applied with the appropriate accuracy — see § 5.7. Since these conditions are imposed on the interface Γ , we must know its location with the same order of accuracy desired for D . In the particular case of the algorithm in this paper, this means 4th order accuracy.

For the reasons above, we adopted a gradient-augmented level set (GALS) representation of the interface, as introduced in [16]. This method allows a simple and completely local 4th order accurate representation of the interface, using Hermite cubics defined everywhere in the domain. The approach also allows the computation of normal vectors in a straightforward and accurate fashion.

5.7. Error analysis.

A naive reading of the discretized system in Eq. (13) suggests that, in order to obtain a fourth order accurate solution u , we need to compute the GFM correction terms $C_{i,j}$ with fourth order accuracy. Thus, from Eq. (14), it would follow that we need to know the correction function D with sixth order accuracy! This is, however, *not correct*, as explained below.

Since we need to compute the correction function D only at grid-points an $\mathcal{O}(h)$ distance away from Γ , it should be clear that errors in the $D_{i,j}$ are equivalent to errors in a and b of the same order. But errors in a and b produce errors of the same order in u — see Eq. (1) and Eq. (2). Hence, if we desire a fourth order accurate solution u , we need to compute the correction terms $D_{i,j}$ with fourth order accuracy only. This argument is confirmed by the convergence plots in Figures 6, 8, and 10.

6. Results.

6.1. General Comments.

In this section we present three examples of computations in 2D using the algorithm introduced in § 5. We solved the Poisson problem in the unit square $[0, 1] \times [0, 1]$ for three different configurations. Each case is defined below in terms of the problem parameters (forcing function f , and jump conditions across Γ), the representation of the interface(s) — using a level set function, and the exact solution (needed to evaluate the errors in the convergence plots). Notice that

1. As explained in Sect. 5, we represent the interface(s) using a GA-LS framework. Hence, the interface is defined by a level set function ϕ , with gradient $\vec{\nabla}\phi = (\phi_x, \phi_y)$ — both of which are carried within the GA-LS framework [16].
2. Below the level set is described via an analytic formula. This formula is converted into the GA-LS representation for the level set, before it is fed into the code. Only this representation is used for the actual computations. This is done so as to test the code's performance under general conditions — where the interface Γ would be known via a level set representation only.
3. Within the GA-LS framework we can, easily and accurately, compute the vectors normal to the interface — anywhere in the domain. Hence, it is convenient to write the jump in the normal derivative, $[u_n]_\Gamma$, in terms of the jump in the gradient of u dotted with the normal to the interface $\hat{n} = (n_x, n_y)$.

6.2. Case 1.

- Problem parameters:

$$\begin{aligned}
f^+(x, y) &= -2\pi^2 \sin(\pi x) \sin(\pi y), \\
f^-(x, y) &= -2\pi^2 \sin(\pi x) \sin(\pi y), \\
[u]_\Gamma &= \sin(\pi x) \exp(\pi y), \\
[u_n]_\Gamma &= \pi [\cos(\pi x) \exp(\pi y) n_x + \sin(\pi x) \exp(\pi y) n_y].
\end{aligned}$$

- Interface level set representation:

$$\phi(x, y) = (x - x_0)^2 + (y - y_0)^2 - r_0^2,$$

where $x_0 = 0.5$, $y_0 = 0.5$, and $r_0 = 0.1$.

- Exact solution:

$$\begin{aligned}
u^+(x, y) &= \sin(\pi x) \sin(\pi y), \\
u^-(x, y) &= \sin(\pi x) [\sin(\pi y) - \exp(\pi y)].
\end{aligned}$$

Figure 5 shows the numerical solution with a fine mesh (193×193 nodes). The discontinuity is captured very sharply, and it causes no oscillations in the solution. Figure 6 shows the behavior of the error in the L_2 and L_∞ norms. As expected, 4th order convergence occurs as the mesh is refined.

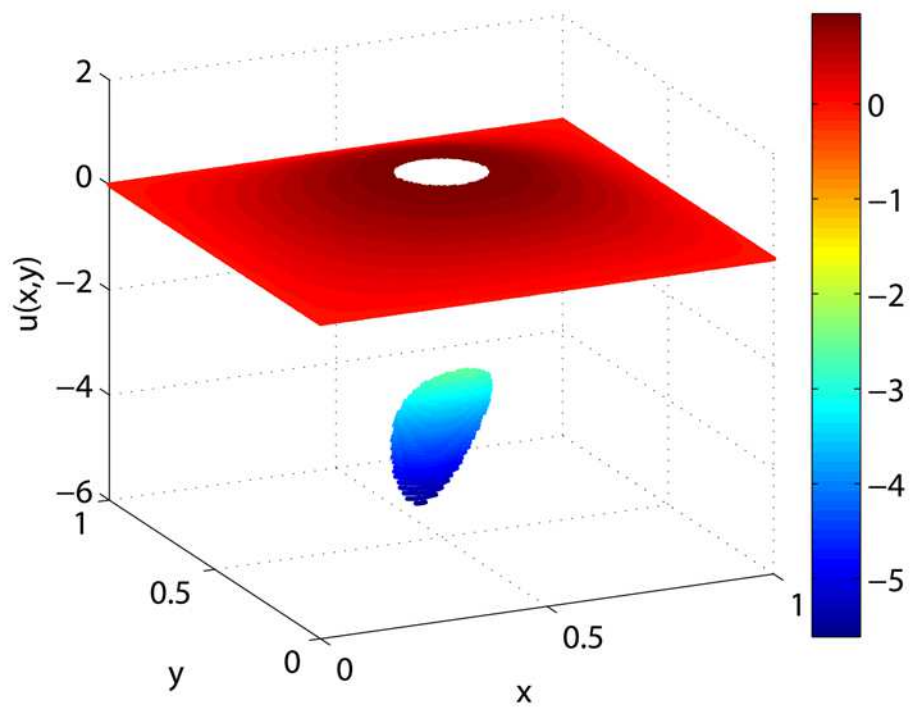


Figure 5: Case 1 - numerical solution with 193×193 nodes.

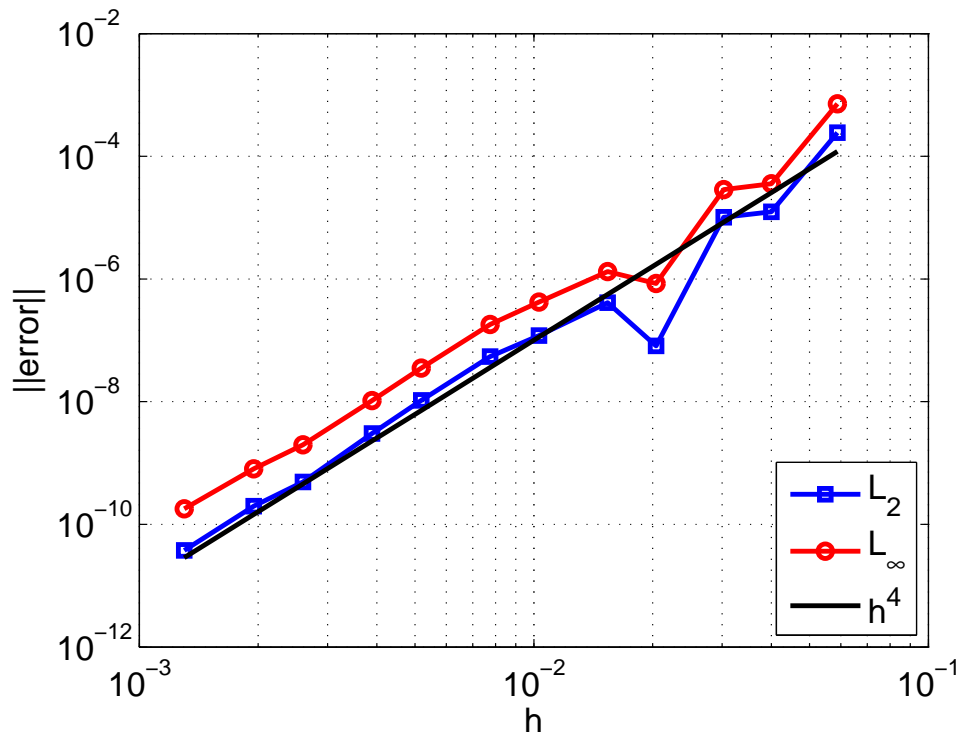


Figure 6: Case 1 - Error behavior in the L_2 and L_∞ norms, versus the theoretical 4th order convergence.

6.3. Case 2.

- Problem parameters:

$$\begin{aligned} f^+(x, y) &= 0, \\ f^-(x, y) &= 0, \\ [u]_\Gamma &= -\exp(x) \sin(y), \\ [u_n]_\Gamma &= -\exp(x) \sin(y) n_x - \exp(x) \cos(y) n_y. \end{aligned}$$

- Interface level set representation:

$$\phi(x, y) = (x - x_0)^2 + (y - y_0)^2 - r^2(\theta),$$

where $r(\theta) = r_0 + \epsilon \sin(5\theta)$, $\theta(x, y) = \arctan\left(\frac{y - y_0}{x - x_0}\right)$, $x_0 = 0.5$, $y_0 = 0.5$, $r = 0.25$, and $\epsilon = 0.05$.

- Exact solution:

$$\begin{aligned} u^+(x, y) &= 0, \\ u^-(x, y) &= \exp(x) \cos(y). \end{aligned}$$

Figure 7 shows the numerical solution with a fine mesh (193×193 nodes). Once again, the overall quality of the solution is very satisfactory. Figure 8 shows the behavior of the error in the L_2 and L_∞ norms. Again, 4th order convergence occurs. However, unlike what happens in case 1, small wiggles are observed in the error plots. This behavior can be explained in terms of the construction of the sets $\Omega_\Gamma^{i,j}$ — see § 5. The approach used to construct $\Omega_\Gamma^{i,j}$ is highly dependent on the way in which the mesh points are placed relative to the interface. Thus, as the mesh is refined, the arrangement of the $\Omega_\Gamma^{i,j}$ can vary quite a lot — specially for a “complicated” interface such as the one in this case. What this means is that, while one can guarantee that the correction function D is obtained with 4th order precision, the proportionality coefficient is not quite constant — it may vary a little from mesh to mesh. This variation is responsible for the small oscillations observed in the convergence plot. Nevertheless, despite these oscillations, the overall convergence is clearly 4th order.

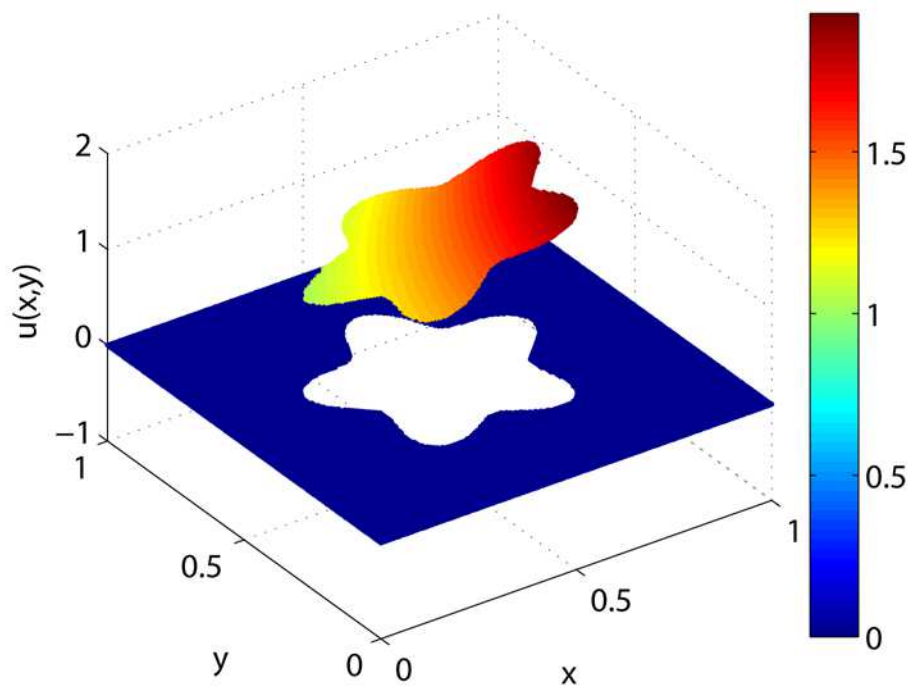


Figure 7: Case 2 - numerical solution with 193×193 nodes.

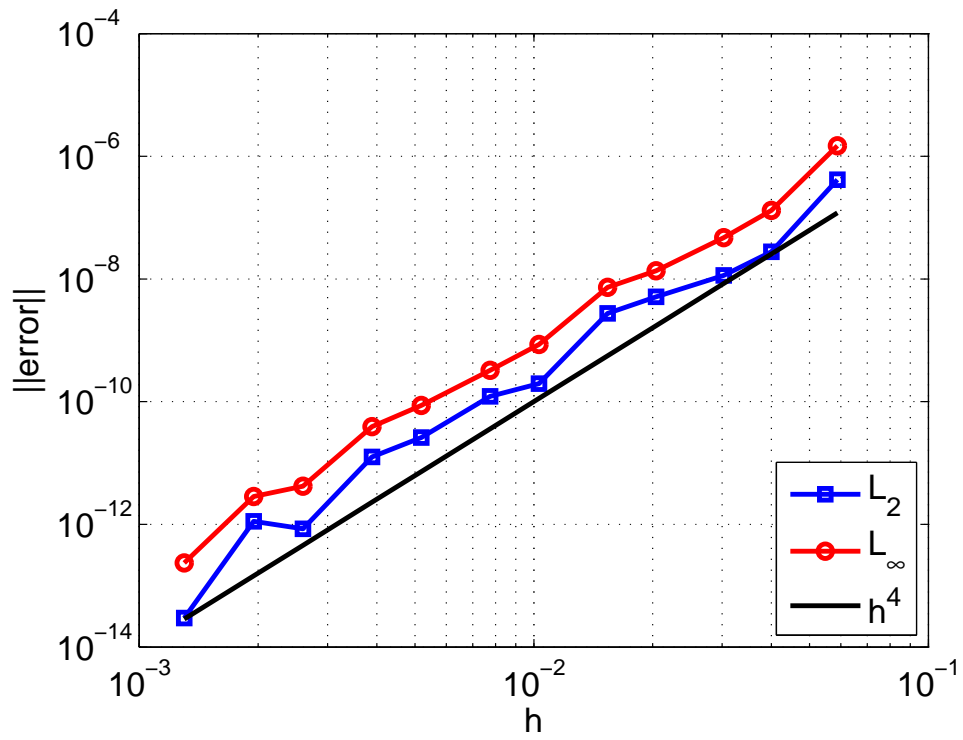


Figure 8: Case 2 - Error behavior in the L_2 and L_∞ norms, versus the theoretical 4th order convergence.

6.4. Case 3.

- Problem parameters:

$$\begin{aligned} f^+(x, y) &= \exp(x) [2 + y^2 + 2 \sin(y) + 4x \sin(y)] , \\ f^-(x, y) &= 40, \\ [u]_\Gamma &= \exp(x) [x^2 \sin(y) + y^2] - 10 (x^2 + y^2) , \\ [u_n]_\Gamma &= \{ \exp(x) [(x^2 + 2x) \sin(y) + y^2] - 20x \} n_x \\ &\quad + \{ \exp(x) [x^2 \cos(y) + 2y] - 20y \} n_y. \end{aligned}$$

- Interface level set representation:

$$\phi(x, y) = [(x - x_1)^2 + (y - y_1)^2 - r_1^2] [(x - x_2)^2 + (y - y_2)^2 - r_2^2] ,$$

where $x_1 = y_1 = 0.25$, $r_1 = 0.15$, $x_2 = y_2 = 0.75$, and $r_2 = 0.1$.

- Exact solution:

$$\begin{aligned} u^+(x, y) &= \exp(x) [x^2 \sin(y) + y^2] , \\ u^-(x, y) &= 10 (x^2 + y^2) . \end{aligned}$$

Figure 9 shows the numerical solution with a fine mesh (193×193 nodes). In this case, there are two circular interfaces in the solution domain. The two regions inside the circles make Ω^- , while the remainder of the domain is Ω^+ . This example shows that the method is general enough to deal with multiple interfaces, keeping the same quality in the solution. Figure 10 shows the behavior of the error in the L_2 and L_∞ norms. Once again we observe 4th order convergence, despite the small oscillations.

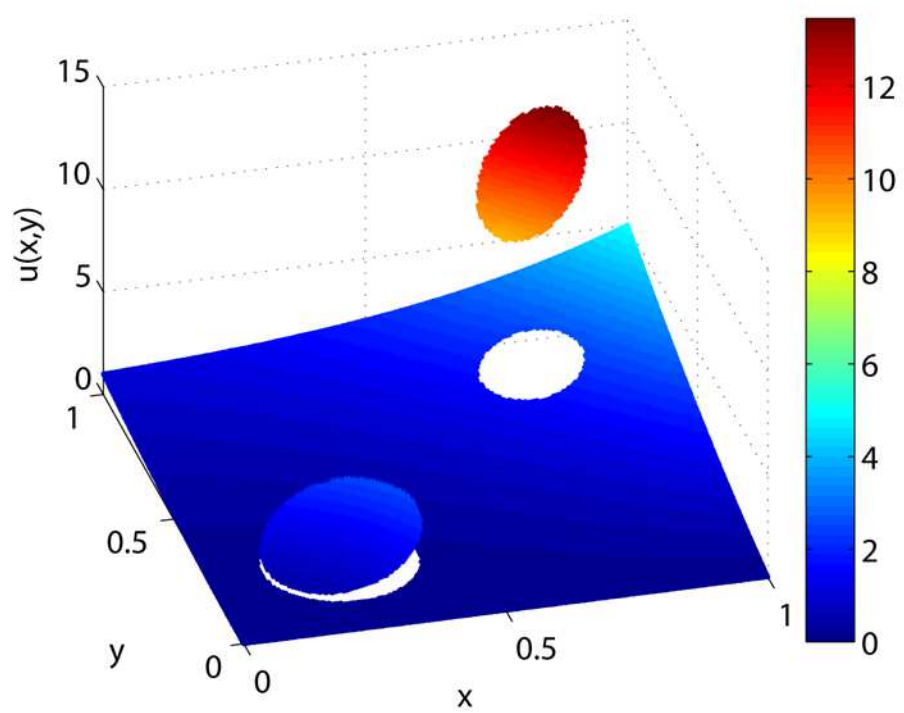


Figure 9: Case 3 - numerical solution with 193×193 nodes.

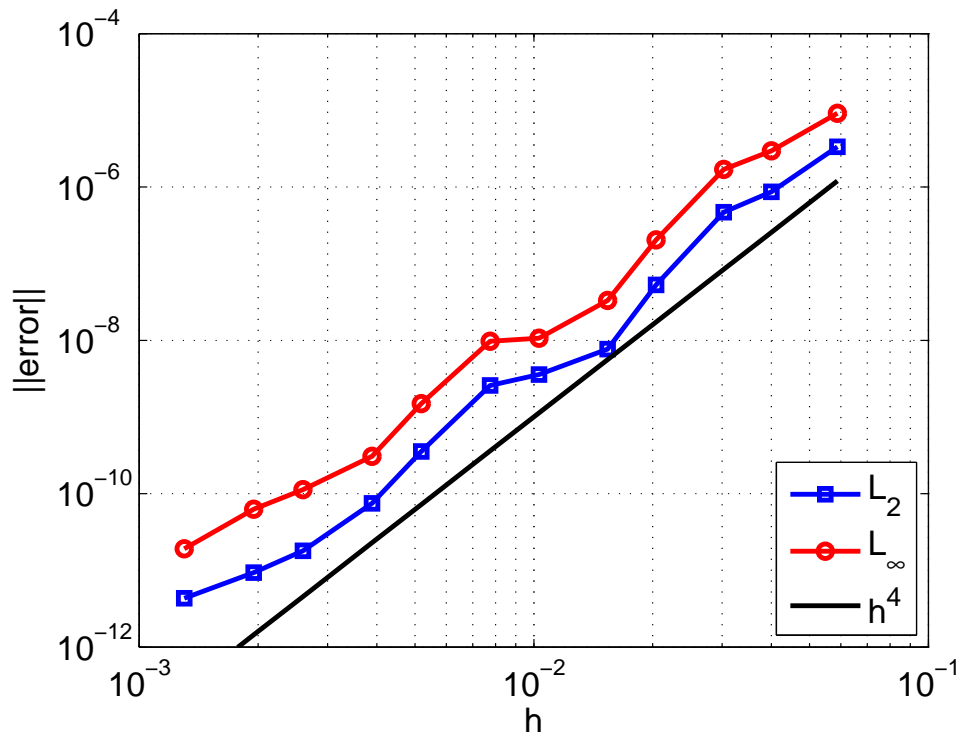


Figure 10: Case 3 - Error behavior in the L_2 and L_∞ norms, versus the theoretical 4th order convergence.

7. Conclusions.

In this paper we have introduced a generalization of the Ghost Fluid Method (GFM), which can be used to obtain (arbitrary) high-order accurate solutions to Poisson problems with interface jump conditions. The generalization is based on extending the correction terms idea of the standard GFM, to that of a correction function defined in a (narrow) band enclosing the interface. This function is the solution of a PDE problem, which can be solved (at least in principle) to any desired order of accuracy. Just as in the original GFM approach, our method allows for the use of standard Poisson solvers. This because (via the correction function) the changes into the problem introduced by the interface jump conditions can be translated into modifications of the standard linear solvers for the Poisson equation, which occur only on the right-hand-side of the discretized linear system of equations.

As an example application, the new method was used to create a 4th-order accurate scheme to solve the Poisson equation with interface jump conditions in 2D. In this scheme, the domain of definition of the correction function is split into many grid size rectangular patches. In each patch the function is represented in terms of a bicubic (with 12 free parameters), and the solution is obtained by minimizing an appropriate (discretized) quadratic functional. The correction function is thus pre-computed, and then is used to modify (in the standard way of the GFM) the right hand side of the Poisson linear system, incorporating the jump conditions into the Poisson solver. We used the standard 4th-order accurate 9-point stencil discretization of the Laplace operator, to thus obtain a 4th order accurate method.

Examples were computed, showing the developed scheme to be robust, accurate, and able to capture discontinuities sharply, without creating spurious oscillations. Furthermore, the scheme is cost effective. First, because it allows the use of standard “black-box” Poisson solvers, which are normally tuned to be extremely efficient. Second, because the additional costs of solving for the correction function scale linearly with the mesh spacing, which means that they become relatively small for large systems.

Finally, we point out that the present method cannot be applied to all the interesting situations where a Poisson problem must be solved with jump discontinuities across an interface. Let us begin by displaying a very general Poisson problem with jump discontinuities at an interface. Specifically,

consider

$$\vec{\nabla} \cdot \left(\beta^+ (\vec{x}) \vec{\nabla} u^+ (\vec{x}) \right) = f^+ (\vec{x}) \quad \text{for } \vec{x} \in \Omega^+, \quad (18a)$$

$$\vec{\nabla} \cdot \left(\beta^- (\vec{x}) \vec{\nabla} u^- (\vec{x}) \right) = f^- (\vec{x}) \quad \text{for } \vec{x} \in \Omega^-, \quad (18b)$$

$$[\alpha u]_\Gamma = a (\vec{x}) \quad \text{for } \vec{x} \in \Gamma, \quad (18c)$$

$$[(\gamma u)_n]_\Gamma + [\eta u]_\Gamma = b (\vec{x}) \quad \text{for } \vec{x} \in \Gamma, \quad (18d)$$

$$u (\vec{x}) = g (\vec{x}) \quad \text{for } \vec{x} \in \partial\Omega, \quad (18e)$$

where we use the notation in § 2 and

7.1 The brackets indicate jumps across the interface, for example:

$$[\alpha u]_\Gamma = (\alpha^+ u^+) (\vec{x}) - (\alpha^- u^-) (\vec{x}) \quad \text{for } \vec{x} \in \Gamma.$$

7.2 The subscript n indicates the derivative in the direction of \hat{n} , the unit normal to the interface Γ pointing towards Ω^+ .

7.3 $\beta^+ > 0$ and f^+ are smooth functions of \vec{x} , defined in the union of Ω^+ and some finite width band enclosing the interface Γ .

7.4 $\beta^- > 0$ and f^- are smooth functions of \vec{x} , defined in the union of Ω^- and some finite width band enclosing the interface Γ .

7.5 $\alpha^\pm > 0$, $\gamma^\pm > 0$, and η^\pm are smooth functions, defined on some finite width band enclosing the interface Γ .

7.6 The Dirichlet boundary conditions in (18e) could be replaced any other standard set of boundary conditions on $\partial\Omega$.

7.7 As usual, the degree of smoothness of the various data functions involved determines how high an order an algorithm can be obtained.

Assume now that $\gamma^\pm = \alpha^\pm$, $\eta^\pm = c \alpha^\pm$ — where c is a constant, and that

$$\left. \begin{aligned} \vec{A} &= \frac{1}{\beta^+} \vec{\nabla} \beta^+ &= \frac{1}{\beta^-} \vec{\nabla} \beta^-, \\ B &= \frac{\alpha^+}{\beta^+} \vec{\nabla} \cdot \left(\beta^+ \vec{\nabla} \left(\frac{1}{\alpha^+} \right) \right) &= \frac{\alpha^-}{\beta^-} \vec{\nabla} \cdot \left(\beta^- \vec{\nabla} \left(\frac{1}{\alpha^-} \right) \right), \end{aligned} \right\} \quad (19)$$

applies in the band enclosing Γ where all the functions are defined.⁵ In this case the methods introduced in this paper can be used to deal with the problem in (18) with minimal alterations. The main ideas carry through, as follows

- 7.a We assume that both u^+ and u^- can be extended across Γ , so that they are defined in some band enclosing the interface.
- 7.b We define the correction function, in the band enclosing Γ where the α^\pm and the u^\pm exist, by $D = \alpha^+(\vec{x}) u^+(\vec{x}) - \alpha^-(\vec{x}) u^-(\vec{x})$.
- 7.c We notice that the correction function satisfies the elliptic Cauchy problem

$$\nabla^2 D + \vec{A} \cdot \vec{\nabla} D + B D = \frac{\alpha^+}{\beta^+} f^+ - \frac{\alpha^-}{\beta^-} f^-, \quad (20)$$

with $D = a$ and $D_n = b - c a$ at the interface Γ .

- 7.d We notice that the GFM correction terms can be written with knowledge of D .

Unfortunately, the conditions in (19) exclude some interesting physical phenomena. In particular, in two-phase flows the case where α^\pm and γ^\pm are constants (but distinct) and $\eta^\pm = 0$ arises. We are currently investigating ways to circumvent these limitations, so as to extend our method to problems involving a wider range of physical phenomena.

Appendix A. Bicubic interpolation.

Bicubic interpolation is similar to bilinear interpolation, and can also be used to represent a function in a rectangular domain. However, whereas bilinear interpolation requires one piece of information per vertex of the rectangular domain, bicubic interpolation requires 4 pieces of information: function value, function gradient, and first mixed derivative (*i.e.* f_{xy}). For completeness, the relevant formulas for bicubic interpolation are presented below.

We use the classical multi-index notation, as in Ref. [16]. Thus, we represent the 4 vertices of the domain using the vector index $\vec{v} \in \{0, 1\}^2$. Namely,

⁵Note that (19) implies that β^+ is a multiple of β^- .

the 4 vertices are $\vec{x}_{\vec{v}} = (x_1^0 + v_1 \Delta x_1, x_2^0 + v_2 \Delta x_2)$, where (x_1^0, x_2^0) are the coordinates of the left-bottom vertex and Δx_i is the length of the domain in the x_i direction. Furthermore, given a scalar function ϕ , the 4 pieces of information needed per vertex are given by

$$\phi_{\vec{\alpha}}^{\vec{v}} = \partial^{\vec{\alpha}} \phi(\vec{x}_{\vec{v}}), \quad (\text{A.1})$$

where both $\vec{v}, \vec{\alpha} \in \{0, 1\}^2$ and

$$\partial^{\vec{\alpha}} = \partial_1^{\alpha_1} \partial_2^{\alpha_2}, \quad \partial_i^{\alpha_i} = (\Delta x_i)^{\alpha_i} \frac{\partial^{\alpha_i}}{\partial x_i^{\alpha_i}}. \quad (\text{A.2})$$

Then the 16 polynomials that constitute the standard basis for the bicubic interpolation can be written in the compact form

$$W_{\vec{\alpha}}^{\vec{v}} = \prod_{i=1}^2 w_{\alpha_i}^{v_i}(\bar{x}_i), \quad (\text{A.3})$$

where $\bar{x}_i = \frac{x - x_i^0}{\Delta x_i}$, and w_{α}^v is the cubic polynomial

$$w_{\alpha}^v(x) = \begin{cases} f(x) & \text{for } v = 0 \text{ and } \alpha = 0, \\ f(1 - x) & \text{for } v = 1 \text{ and } \alpha = 0, \\ g(x) & \text{for } v = 0 \text{ and } \alpha = 1, \\ -g(1 - x) & \text{for } v = 1 \text{ and } \alpha = 1, \end{cases} \quad (\text{A.4})$$

where $f(x) = 1 - 3x^2 + 2x^3$ and $g(x) = x(1 - x)^2$.

Finally, the bicubic interpolation of a scalar function ϕ is given by the following linear combination of the basis functions:

$$\mathcal{H}(\vec{x}) = \sum_{\vec{v}, \vec{\alpha} \in \{0, 1\}^2} W_{\vec{\alpha}}^{\vec{v}} \phi_{\vec{\alpha}}^{\vec{v}} \quad (\text{A.5})$$

As defined above (standard bicubic interpolation), 16 parameters are needed to determine the bicubic. However, in Ref. [16] a method (“cell-based approach”) is introduced, that reduces the number of degrees of freedom to 12, without compromising accuracy. This method uses information from the first derivatives to obtain approximate formulae for the mixed derivatives. In the present work, we adopt this cell-based approach.

Acknowledgements

The authors would like to acknowledge the National Science Foundation support — this research was partially supported by grant DMS0813648. In addition, the first author acknowledges the support by Coordenação de Aperfeiçoamento de Pessoal de Nível Superior (CAPES – Brazil) and the Fulbright Commission through grant BEX 2784/06-8. The authors would also like to acknowledge many helpful conversations with Prof. B. Seibold at Temple University.

References

References

- [1] C. S. Peskin, Numerical analysis of blood flow in the heart, *Journal of Computational Physics* 25 (3) (1977) 220–252. doi:10.1016/0021-9991(77)90100-0.
- [2] M. Sussman, P. Smereka, S. Osher, A level set approach for computing solutions to incompressible two-phase flow, *Journal of Computational Physics* 114 (1) (1994) 146–159. doi:10.1006/jcph.1994.1155.
- [3] R. J. LeVeque, Z. Li, The immersed interface method for elliptic equations with discontinuous coefficients and singular sources, *SIAM Journal on Numerical Analysis* 31 (4) (1994) 1019–1044. doi:10.1137/0731054.
- [4] R. J. LeVeque, Z. Li, Immersed interface methods for Stokes flow with elastic boundaries or surface tension, *SIAM Journal on Scientific Computing* 18 (3) (1997) 709–735. doi:10.1137/S1064827595282532.
- [5] H. Johansen, P. Colella, A Cartesian grid embedded boundary method for Poisson’s equation on irregular domains, *Journal of Computational Physics* 147 (1) (1998) 60–85. doi:10.1006/jcph.1998.5965.
- [6] R. P. Fedkiw, T. Aslam, S. Xu, The ghost fluid method for deflagration and detonation discontinuities, *Journal of Computational Physics* 154 (2) (1999) 393–427. doi:10.1006/jcph.1999.6320.
- [7] R. P. Fedkiw, T. Aslam, B. Merriman, S. Osher, A non-oscillatory Eulerian approach to interfaces in multimaterial flows (the ghost fluid method), *Journal of Computational Physics* 152 (2) (1999) 457–492. doi:10.1006/jcph.1999.6236.

- [8] M. Kang, R. P. Fedkiw, X.-D. Liu, A boundary condition capturing method for multiphase incompressible flow, *Journal of Scientific Computing* 15 (2000) 323–360. doi:10.1023/A:1011178417620.
- [9] X.-D. Liu, R. P. Fedkiw, M. Kang, A boundary condition capturing method for Poisson’s equation on irregular domains, *Journal of Computational Physics* 160 (1) (2000) 151–178. doi:10.1006/jcph.2000.6444.
- [10] M.-C. Lai, C. S. Peskin, An immersed boundary method with formal second-order accuracy and reduced numerical viscosity, *Journal of Computational Physics* 160 (2) (2000) 705–719. doi:10.1006/jcph.2000.6483.
- [11] Z. Li, M.-C. Lai, The immersed interface method for the Navier-Stokes equations with singular forces, *Journal of Computational Physics* 171 (2) (2001) 822–842. doi:10.1006/jcph.2001.6813.
- [12] D. Q. Nguyen, R. P. Fedkiw, M. Kang, A boundary condition capturing method for incompressible flame discontinuities, *Journal of Computational Physics* 172 (1) (2001) 71–98. doi:10.1006/jcph.2001.6812.
- [13] L. Lee, R. J. LeVeque, An immersed interface method for incompressible Navier-Stokes equations, *SIAM Journal on Scientific Computing* 25 (3) (2003) 832–856. doi:10.1137/S1064827502414060.
- [14] F. Gibou, L. Chen, D. Nguyen, S. Banerjee, A level set based sharp interface method for the multiphase incompressible Navier-Stokes equations with phase change, *Journal of Computational Physics* 222 (2) (2007) 536–555. doi:10.1016/j.jcp.2006.07.035.
- [15] L. N. Trefethen, D. Bau, *Numerical Linear Algebra*, SIAM: Society for Industrial and Applied Mathematics, 1997.
- [16] J.-C. Nave, R. R. Rosales, B. Seibold, A gradient-augmented level set method with an optimally local, coherent advection scheme, *Journal of Computational Physics* 229 (10) (2010) 3802 – 3827. doi:10.1016/j.jcp.2010.01.029.

- [17] A. Mayo, The fast solution of Poisson's and the biharmonic equations on irregular regions, *SIAM Journal on Numerical Analysis* 21 (2) (1984) 285–299. doi:10.1137/0721021.
- [18] H. S. Udaykumar, R. Mittal, W. Shyy, Computation of solid-liquid phase fronts in the sharp interface limit on fixed grids, *Journal of Computational Physics* 153 (2) (1999) 535–574. doi:10.1006/jcph.1999.6294.
- [19] F. Gibou, R. P. Fedkiw, L.-T. Cheng, M. Kang, A second-order-accurate symmetric discretization of the Poisson equation on irregular domains, *Journal of Computational Physics* 176 (1) (2002) 205–227. doi:10.1006/jcph.2001.6977.
- [20] Z. Jomaa, C. Macaskill, The embedded finite difference method for the Poisson equation in a domain with an irregular boundary and Dirichlet boundary conditions, *Journal of Computational Physics* 202 (2) (2005) 488–506. doi:10.1016/j.jcp.2004.07.011.
- [21] F. Gibou, R. Fedkiw, A fourth order accurate discretization for the Laplace and heat equations on arbitrary domains, with applications to the Stefan problem, *Journal of Computational Physics* 202 (2) (2005) 577–601. doi:10.1016/j.jcp.2004.07.018.
- [22] H. Chen, C. Min, F. Gibou, A supra-convergent finite difference scheme for the Poisson and heat equations on irregular domains and non-graded adaptive Cartesian grids, *Journal of Scientific Computing* 31 (1) (2007) 19–60. doi:10.1007/s10915-006-9122-8.
- [23] J. A. Sethian, J. Strain, Crystal growth and dendritic solidification, *Journal of Computational Physics* 98 (2) (1992) 231–253. doi:10.1016/0021-9991(92)90140-T.
- [24] S. Chen, B. Merriman, S. Osher, P. Smereka, A simple level set method for solving Stefan problems, *Journal of Computational Physics* 135 (1) (1997) 8–29. doi:10.1006/jcph.1997.5721.